

New SDW phases in quasi-one-dimensional systems dimerized in the transverse direction

Dražen Zanchi

*Laboratoire de Physique Théorique et Hautes Energies. Universités
Paris VI Pierre et Marie Curie – Paris VII Denis Diderot,
2 Place Jussieu, 75252 Paris Cédex 05, France.*

Aleksa Bjeliš

*Department of Physics, Faculty of Science,
University of Zagreb, POB 162, 10001 Zagreb, Croatia*

Abstract

The spin density wave instabilities in the quasi-one-dimensional metal $(\text{TMTSF})_2\text{ClO}_4$ are studied in the framework a matrix random phase approximation for intra-band and inter-band order parameters. Depending on the anion ordering potential V which measures the lattice doubling in the transverse direction, two different instabilities are possible. The SDW_0 state at low values of V is antiferromagnetic in b direction and has the critical temperature that decreases rapidly with V . The degenerated states SDW_\pm , stable at higher values of V , are superpositions of two magnetic orders, each one on its subfamily of chains. As V increases the ratio between two components of SDW_\pm tends to zero and the critical temperature increases asymptotically towards that of SDW instability for a system having perfect nesting and no anion order. At intermediate V , i.e. between the phases SDW_0 and SDW_\pm , the metallic state can persist down to $T = 0$.

PACS 75.10.Lp, 75.10.Fv, 74.70.Kn

Among the quasi-one-dimensional systems $(\text{TMTSF})_2X$ with the generic name Bechgaard salts the material $X=\text{ClO}_4$ has a particular status. If relaxed, it is a superconductor at ambient pressure and develops a field-induced spin-density-wave (FISDW) cascade for the magnetic fields B above 3 Tesla, well above the critical field for superconductivity. At even higher values of B it possesses a still controversial type of SDW ordering.[1] If the sample is cooled more rapidly, the SDW order can persist even down to zero magnetic field. The critical temperature of this zero-field transition increases with the cooling rate up to the value of about 5.5 K for quenched samples.[2, 3] It is believed that this strong dependence of the SDW ordering on the cooling rate and its absence in carefully relaxed samples are related to the fact that $(\text{TMTSF})_2\text{ClO}_4$ in its ground state acquires a long range order of anion molecules ClO_4 . This ordering sets up at the temperatures up to about 24K, inducing a doubling of the unit cell perpendicularly to chains, with the new lattice constant $d = 2b$, b being the inter-chain distance, as shown on Fig. 1. By varying the cooling rate one realizes a tunable unit cell doubling which in turn strongly influences the SDW ordering.

The usual and the most direct measure of this doubling on the electron band properties is the band splitting V of α and β sub-families of chains (Fig. 1).[4] We take that $V = -|V|$ on α chains and $V = |V|$ on β chains. It was already pointed out that due to this splitting the two SDWs shown on Figs. 1(a) and 1(b) are in competition.[1, 5, 6] Realizing that these SDWs cannot be treated independently (i.e. additively) as it was done in the existing bibliography, we develop a generalized matrix method within the random phase approximation (RPA). In this Letter we concentrate on $(\text{TMTSF})_2\text{ClO}_4$ in the absence of magnetic field, and determine the phase diagram in whole range of values of the band splitting V , particularly for the physically relevant intermediate values, not properly covered in the previous analyses.

As it is well known the Coulomb interaction between electrons leads to a SDW ordering via the mechanism of Fermi surface nesting.[7] If the chains were equivalent the nesting would lead to a SDW order with the magnetization modulation characterized by the wave-vector $(2k_F, \pi/b)$ as shown on Fig. 1(a). One can imagine that in the limit of strong dimerization the nesting mechanism is again in action, but now separately for bands of α and β sub-families of chains from Fig. 1, and conclude that the critical temperature for each subfamily

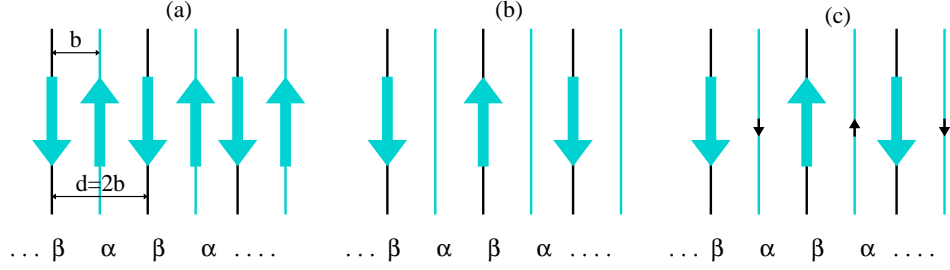


FIG. 1: Magnetic pattern in direction perpendicular to chains for three characteristic cases of transverse SDW modulation: (a) the limit of weak anion potential V with $p = \pi/b$; (b) the limit of large V with $p = \pi/d$; (c) V/t_b moderate with $p = \pi/d$ transverse SDW order.

is of the same order as that for equivalent chains provided the new nesting is again (close to) perfect. The new SDW then has doubled period $2d = 4b$ in the b direction, as shown on Fig.1(b) for the subfamily β . Our analysis confirms that this indeed happens in the limit of large anion potential, $V \gg t_b$, where t_b is the interchain hopping integral. However for intermediate values of V the situation is more subtle due to the mixing of two SDWs. There, a new type of SDW dominates the response. It is a combination of two SDW orders on two different sublattices, each one forming an antiferromagnetic pattern in b direction, as shown schematically on Fig. 1(c). We show that then the critical temperature is reduced or even completely suppressed.

All modulations from Fig. 1 can be followed in terms of homogeneous and alternating SDW amplitudes defined on the dimerized lattice

$$\begin{aligned} \mathbf{M}_h(x, n) &= \mathbf{M}_\alpha(x, nd) + \mathbf{M}_\beta(x, nd + d/2) = \frac{1}{2}[\mathbf{M}_{11}(x, n) + \mathbf{M}_{22}(x, n)] \\ \mathbf{M}_a(x, n) &= \mathbf{M}_\alpha(x, nd) - \mathbf{M}_\beta(x, nd + d/2) = \frac{1}{2}[\mathbf{M}_{12}(x, n) + \mathbf{M}_{21}(x, n)], \end{aligned} \quad (1)$$

represented for later convenience in terms of SDW amplitudes on $\alpha(\beta)$ chains $\mathbf{M}_{\alpha(\beta)} = c_{+\alpha(\beta)}^\dagger \sigma c_{-\alpha(\beta)}$, and in terms of $\mathbf{M}_{ij} = \Psi_{+,i}^\dagger \sigma \Psi_{-,j}$ (with $i, j = 1, 2$) which are the SDW amplitudes in terms of the bond/antibond states

$$\Psi_{f,1(2)}(x, n) = \frac{1}{\sqrt{2}}[c_{f,\alpha}(x, nd) \pm c_{f,\beta}(x, nd + d/2)], \quad (2)$$

with $f = +, -$. Here $c_{\pm\alpha(\beta)}$ are two component field operators for the right (left) Fermi sheet, and σ is the Pauli operator in the spin space. Note that operators defined in the

bond/antibond basis (Ψ , \mathbf{M}_{ij} and $\mathbf{M}_{h(a)}$) depend only on the cell index n , while the local operators c and $\mathbf{M}_{\alpha(\beta)}$ depend also on the position within the unit cell. In particular this means that $c_{f,\alpha}(x, nd + d/2) = c_{f,\beta}(x, nd) = 0$ and $\mathbf{M}_\alpha(x, nd + d/2) = \mathbf{M}_\beta(x, nd) = 0$.

Below T_c both \mathbf{M}_h and \mathbf{M}_a can attain non-zero mean values, with some specific common wave vector $\mathbf{q} = (k, p)$ and with the common orientation along some easy axis, say \hat{z} . The staggered magnetization is then

$$m_z(x, R_\perp) = (\Delta_h \pm \Delta_a) \cos [(2k_F + k)x + pnd], \quad (3)$$

where the upper and lower sign stay for $\alpha (R_\perp = nd)$ and $\beta (R_\perp = nd + d/2)$ chains respectively, and $\Delta_{h/a}$ are the mean values of the critical Fourier components (k, p) of $\mathbf{M}_{h/a}$. With $\Delta_a \neq 0$, $\Delta_h = 0$ and $p = 0$ we get a simple antiferromagnetic order in b direction [Fig. 1(a)], like in the case of indistinguishable chains. We call this state SDW_0 . Another limit with doubled periodicity [Fig. 1(b)] is realized for $\Delta_h = \Delta_a$ or $\Delta_h = -\Delta_a$ with $p = \pi/d$. In this case the SDW with antiferromagnetic modulation in the transverse direction can be realized either on the chains α or on the chains β , each ordering having its own longitudinal modulation, with respective wave-numbers $2k_F + k_1$ and $2k_F - k_1$.

The intermediate ordering from Fig.1(c) is realized for $|\Delta_h/\Delta_a| > 1$. The corresponding ordered states with larger $(2k_F + k_1)$ and smaller $(2k_F - k_1)$ value of the longitudinal wave number will be denoted by SDW_+ and SDW_- respectively. Fig. 1(c) shows the ordering with $\Delta_h/\Delta_a < -1$, i. e. with the larger SDW amplitude on β chains. Its longitudinal modulation has the wavenumber $2k_F - k_1$.

Written in terms of the Fourier transforms of the operators (1) in the perpendicular (b) direction with the Brillouin zone defined by $(-\pi/d < q < \pi/d)$, the interaction term of the Hamiltonian reads

$$H_I = -\frac{U}{2N} \int dx \sum_q [\mathbf{M}_h^\dagger(x, q)\mathbf{M}_h(x, q) + \mathbf{M}_a^\dagger(x, q)\mathbf{M}_a(x, q)], \quad (4)$$

while the band contribution, written in terms of bond/antibond operators defined by eq.(2), reads

$$H_0 = \frac{1}{2N} \sum_\sigma \sum_{p=-\pi/d}^{\pi/d} \int dx \Psi^\dagger(x, p) \left[iv_F \rho_3 \partial_x + 2\tau_3 t_b \cos \frac{pd}{2} + 2t'_b \cos pd - V\tau_1 \right] \Psi(x, p). \quad (5)$$

Here $\Psi^\dagger(x, p) = (\Psi_1^\dagger(x, p), \Psi_2^\dagger(x, p))$, ρ 's and τ 's are Pauli matrices in left-right and bond-antibond indices respectively, t'_b is the parameter which introduces an imperfect nesting in the absence of the anion ordering, and $2N$ is the total number of chains. Also, being interested only in the SDW channel, we keep here only the forward part of the presumably local (intrachain) electron-electron coupling in H_I , omitting also the weak Umklapp term due to the existing slight lattice dimerization along the chain.

Following the above qualitative arguments, it appears natural to construct the RPA formalism in the $\mathbf{M}_{a,h}$ basis. However, although the interaction term H_I is separated in \mathbf{M}_a and \mathbf{M}_h , these SDW amplitudes are coupled through the non-diagonal part of the kinetic term (5), induced by anion ordering. Since the electron propagators in the bond-antibond basis are not diagonal, the RPA equations for $\mathbf{M}_{a(h)}$ amplitudes are also coupled. One gets the static SDW susceptibility in the form of a 2x2 matrix,

$$[\chi(\mathbf{q})] \equiv \left(\langle M_i(\mathbf{q}) M_j^\dagger(\mathbf{q}) \rangle \right) = D^{-1} \begin{pmatrix} (1 - U\chi_{aa})\chi_{hh} + U(\chi_{ha})^2 & \chi_{ha} \\ \chi_{ha} & (1 - U\chi_{hh})\chi_{aa} + U(\chi_{ha})^2 \end{pmatrix}, \quad (6)$$

where indices i and j stand for h and a , M_i is the projection of \mathbf{M}_i onto the spin quantization axis, $D(\mathbf{q}) \equiv (1 - U\chi_{hh})(1 - U\chi_{aa}) - U^2(\chi_{ha})^2$, and χ_{hh}, χ_{aa} and $\chi_{ah} = \chi_{ha}$ are corresponding bare (Hartree-Fock) susceptibilities.

The diagonalization of the matrix (6) leads to

$$[\chi(\mathbf{q})] = \text{diag} \left(\frac{\tilde{\chi}_1}{1 - U\tilde{\chi}_1}, \frac{\tilde{\chi}_2}{1 - U\tilde{\chi}_2} \right), \quad (7)$$

with

$$\tilde{\chi}_{1/2} = \frac{1}{2} \left[\chi_{aa} + \chi_{hh} \pm \sqrt{(\chi_{aa} - \chi_{hh})^2 + 4(\chi_{ha})^2} \right]. \quad (8)$$

The SDW instability takes place for

$$1 - U\tilde{\chi}_1(T_c, \mathbf{q}_c) = 0, \quad (9)$$

\mathbf{q}_c being the wave vector at which $\tilde{\chi}_1(\mathbf{q})$ has the maximum. The corresponding ratio of two SDW order parameters from eq.(3) is

$$\frac{\Delta_h}{\Delta_a} = \pm \sqrt{\frac{1 - \eta}{\eta}}, \quad (10)$$

with

$$\eta = \frac{1}{2} \left[1 + \frac{\chi_{aa} - \chi_{hh}}{\sqrt{(\chi_{aa} - \chi_{hh})^2 + 4(\chi_{ha})^2}} \right]. \quad (11)$$

The sign ambiguity in eq.(10) comes from the freedom of choice of the unit cell: (α, β) or (β, α) .

It is convenient for further considerations to write the critical SDW susceptibility $\tilde{\chi}_1$ in the form $\tilde{\chi}_1(k, p) = \frac{1}{2\pi v_F} [\ln \frac{\epsilon}{T} + \chi_{\text{res}}(k, p)]$, where χ_{res} is always negative and contains all corrections to the pure logarithm. It can be derived after passing to the electron basis that diagonalizes the kinetic part (5) of the Hamiltonian. The result is

$$\begin{aligned} \chi_{\text{res}}(k, p) = & \Psi\left(\frac{1}{2}\right) - \frac{1}{4} \left\langle \sum_{X,Y} (1 + 4XY\alpha\beta\alpha_p\beta_p) \Psi_{XY} \right\rangle \\ & + \frac{1}{4} \left[\left\langle (\alpha^2 - \beta^2)(\alpha_p^2 - \beta_p^2) \sum_{X,Y} XY \Psi_{XY} \right\rangle^2 + 16 \left\langle \alpha\beta \sum_{X,Y} X \Psi_{XY} \right\rangle^2 \right]^{1/2}. \end{aligned} \quad (12)$$

Here $\langle \dots \rangle$ means the average along the transverse momentum $(-\pi/d < p' < \pi/d)$, Ψ is di-gamma function, X and Y take the values ± 1 , $\Psi_{XY} \equiv \Re \Psi(\frac{1}{2} + iQ_{XY})$ with $Q_{XY} \equiv \frac{1}{4\pi T} \left[v_F k + 2t'_b [\cos(p' + p) + \cos p'] - X\Delta(p') - Y\Delta(p' + p) \right]$, and $\Delta(p) \equiv \sqrt{V^2 + [2t_b \cos(\frac{pd}{2})]^2}$. α and β are the coefficients defining the unitary transformation that diagonalizes the band term (5),

$$\begin{Bmatrix} \alpha(p') \\ \beta(p') \end{Bmatrix} = \sqrt{\frac{1}{2} \left[1 \pm \frac{2t_b |\cos(\frac{p'd}{2})|}{\Delta(p')} \right]}, \quad (13)$$

with the convention $\alpha_p \equiv \alpha(p' + p)$ used to shorten writing in eq. (12). The corresponding dispersions of two sub-bands are given by

$$E_{\pm f}(k, p) = f v_F k + 2t'_b \cos(pd) \pm \Delta(p). \quad (14)$$

The critical temperature is now the solution of the equation $\ln \frac{T_c}{T_c^0} = \chi_{\text{res}}(T_c, V, t_b, t'_b; \mathbf{q}_c)$, where \mathbf{q}_c is always chosen to maximize χ_{res} , and $T_c^0 \equiv T_c(V = 0, t'_b = 0) = \epsilon \exp(-\frac{\pi v_F}{U})$ is the t_b -independent critical temperature for the asymptotic case of perfect nesting ($t'_b = 0$) and vanishing anion order ($V = 0$); ϵ is a constant of the order of the bandwidth.

The wave vector dependence of $\chi_{\text{res}}(k, p)$ is illustrated on Fig. 2a, in which we chose $t'_b/t_b = 0.1, V/t_b = 1.2$, and a very low temperature ($T/t_b = 0.0004$) in order to make the

whole fine structure of this dependence visible. There is one peak at $\mathbf{q}_0 = (4t'_b/v_F, 0)$, and two mirroring peak structures positioned approximately at $\mathbf{q}_\pm = (k^\pm, \pi/d)$, with k^\pm to be specified below.

The peak at \mathbf{q}_0 corresponds to the phase SDW_0 . It reproduces the standard SDW instability appearing in the absence of the anion ordering.[1, 7] Indeed it dominates over the peaks at \mathbf{q}_\pm for low values of V/t_b , as it will be shown later in the discussion of the whole phase diagram. If in addition the temperature is not too much lower than t'_b this peak is smeared and is simply shifted to $k = 0$, i.e. to the SDW_0 with a pure $2k_F$ longitudinal modulation. One gets the two-band version of the well-known imperfect nesting induced commensurate–incommensurate transition [7], with $\eta \approx 1$, i. e. with the SDW_0 order very close to an antiferromagnet in the transverse direction as shown on Fig. 1(a). Here SDW_0 is stabilized as an interband process: the wave vector $\mathbf{Q}_0 = 2k_F\hat{a} + \mathbf{q}_0$ is the best nesting vector connecting the left Fermi sheet of the sub-band “+” with the right Fermi sheet of the sub-band “-”, whose dispersions are given by eq. (14). Note that in this range of wave vectors the anion potential V is also, beside the original imperfect nesting t'_b , the source of deviation from the purely logarithmic susceptibility. It becomes clear from the expression (12) which after putting $k = 0$, $p = 0$ and $t'_b = 0$ reads

$$\chi_{\text{res}}(0, 0) \approx \left\langle \frac{V^2}{V^2 + [2t_b \cos(\frac{p'd}{2})]^2} \left[\Psi\left(\frac{1}{2}\right) - \Re \Psi\left(\frac{1}{2} + \frac{i\sqrt{V^2 + [2t_b \cos(\frac{p'd}{2})]^2}}{2\pi T}\right) \right] \right\rangle. \quad (15)$$

Note that one gets the same expression after putting $k = 0$, $p = 0$ and $t'_b = 0$ into the result of Miyazaki et al [11]. For this particular case the off-diagonal element of the SDW susceptibility (6) vanishes, so that the matrix approach reduces to the standard scalar one.

The peak at \mathbf{q}_+ on Fig. 2a is in fact a plateau delimited on the axe $p = \pi/d$ by the wave numbers $k_1^+ = (\sqrt{V^2 + 4t_b^2} + V)/v_F$ and $k_2^+ = 2\sqrt{V^2 + 2t_b^2}/v_F$, as shown by the enlarged picture of this part of Brillouin zone on Fig.2(b). This range of wave vectors is the intra-band nesting range for the sub-band E_- in eq.(14). Equivalently, the range \mathbf{q}_- has the same role for the sub-band E_+ . The complete degeneracy of these two ranges would be raised after inclusion of higher corrections to the longitudinal linear dispersion in the one-electron spectrum assumed here. E. g. for the band–filling lower than one half the dominant SDW ordering is realized on the subfamily of chains which is higher in energy because it has a

lower Fermi velocity and, consequently, a higher density of states. In that case, the minus sign is to be chosen in eq. (10).

The wave numbers k_1^+ and k_2^+ delimit the region where after the translation by the wave vector $\mathbf{Q}_+ = 2k_F\hat{\mathbf{a}} + \mathbf{q}_+$ the left and right Fermi sheets cross each other, from the region where these sheets are not in contact. The difference $\Delta k = k_1^+ - k_2^+$ measures the strength of effective imperfect nesting for the intraband SDW_+ ordering. In the limit of large anion splitting, $V \gg t_b$, it reduces to $v_F\Delta k \approx t_b^4/V^3 \equiv 8\epsilon_{\text{eff}}$. In the language of the standard nesting model for SDW ordering [7] ϵ_{eff} is the effective next-nearest neighbor hopping in the diagonalized Hamiltonian, while t'_b takes over the role of an effective nearest neighbor hopping, i. e. it does not affect the perfect nesting for SDW_+ and SDW_- . This is in contrast to the interband SDW_0 ordering for which finite t'_b introduces an imperfect nesting, and t_b keeps the nesting perfect. For temperatures $T > \epsilon_{\text{eff}}$ the fine plateau on Fig.2 is washed away and rounded to a single maximum at $p = \pi/d$ and $k_1 \approx 2V(1 + t_b^2/V^2)/v_F$ for $V \gg t_b$.

The magnetic pattern of the phase SDW_- is represented on Fig.1(c) for $\eta \approx 0.3$. As V increases the parameter η approaches the value $1/2$ from below, i. e. the SDW_- modulation in the transverse direction is closer and closer to the antiferromagnetic form from Fig.1(b). Furthermore, in the limit $t_b/V \rightarrow 0$ the nonlogarithmic term in eq.(12) reduces to $\chi_{\text{res}}(\pm k_1, \pi/d) \approx \frac{t_b^2}{V^2} \left[\Psi\left(\frac{1}{2}\right) - \Re\Psi\left(\frac{1}{2} + \frac{iV}{2\pi T}\right) \right]$, i. e. the critical temperature approaches its asymptotic value for the perfect nesting, T_c^0 . Note that in this limit $\chi_{\text{res}}(0, 0)$ tends to $\Psi(\frac{1}{2}) - \Re\Psi(\frac{1}{2} + \frac{iV}{2\pi T})$, as is seen from eq.(15), i. e. on Fig. 2a the peaks at \mathbf{q}_{\pm} dominate over that at \mathbf{q}_0 .

The phase diagram that results from the above considerations is shown in Fig.3 in which the Coulomb coupling strength is parametrized by the perfect nesting critical temperature T_c^0 . Fig.3a represents the case with $t'_b = 0$. Then the low- V (SDW_0) and high- V (SDW_{\pm}) phases are clearly separated by a "valley" in the range of intermediate values of V . The case with the imperfect nesting is illustrated on Fig.3(b) for $t'_b = 0.0375t_b$.

The representatives of $T_c(V)$ dependences for the perfect nesting and highly imperfect nesting cases, as well as the V -dependence of the parameter η , are shown on Fig.3(c). The Coulomb interaction is chosen to give $T_c^0 = 0.0108 \times 4t_b$ (i. e. $T_c^0 = 13K$ for $t_b = 300K$). As was already pointed out, the critical temperature for SDW_{\pm} phases, and the parameter η as

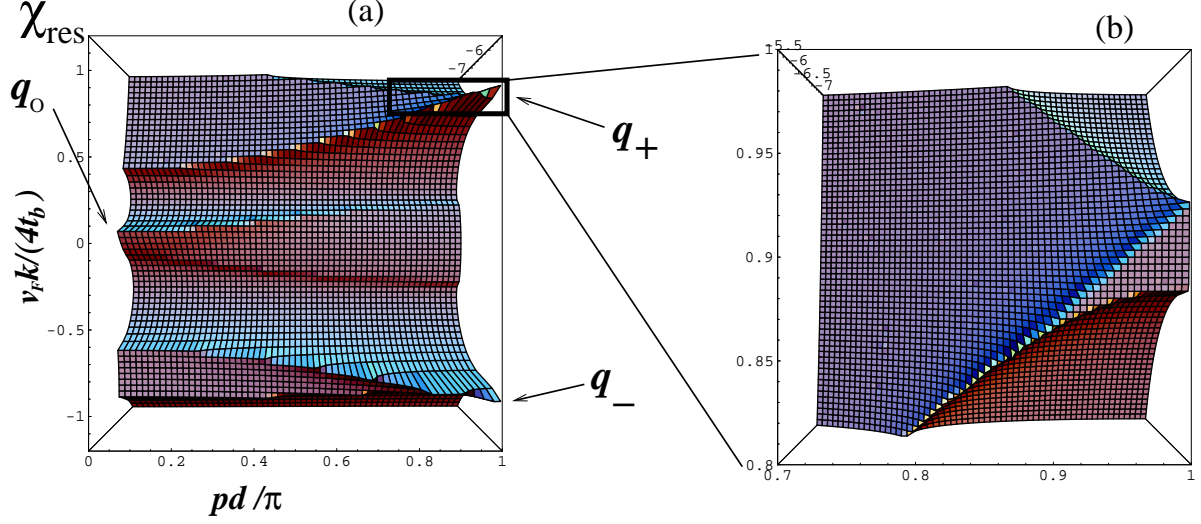


FIG. 2: The quantity χ_{res}

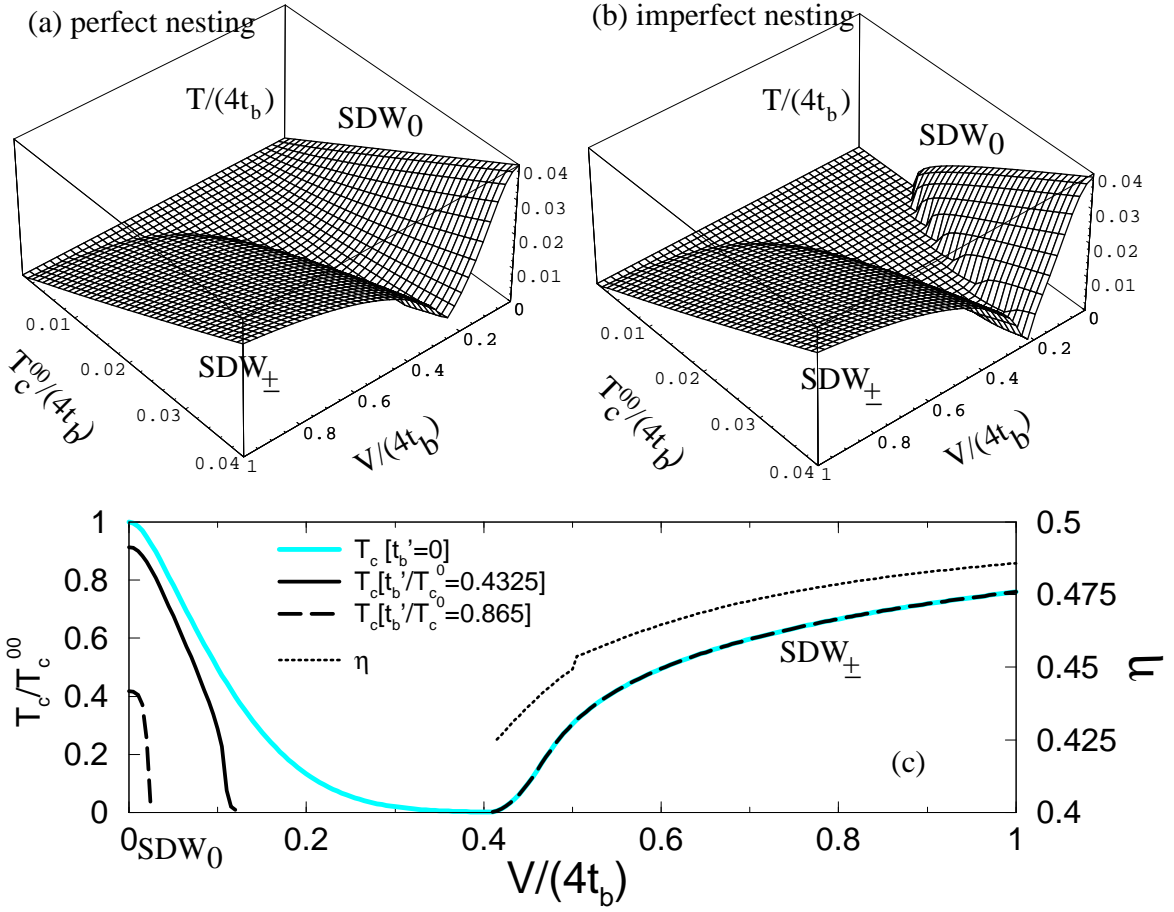


FIG. 3: The phase diagram. Small discontinuity in the η vs $V/4t_b$ dependence is caused by the jump from k_2^+ to $(k_1^+ + k_2^+)/2$ in the Stoner criterion (9).

well [right side of Fig.3(c)] are not affected by t'_b . On contrary, the critical temperature for phase SDW_0 is very sensitive on the parameter t'_b , and is completely suppressed for $t'_b \approx T_c^0$.

An attempt to make the correspondence of our phase diagram with the experimental one for $(TMTSF)_2ClO_4$ cannot be pursued without ambiguities. The main problem is a reliable choice of the value for the parameter t'_b (beside the more or less well established values for other parameters, $t_b = 300K$ and $T_c^0 = 13K$. The value $t'_b = 11.25K$ is suggested from the experiments in quenched system [2] under the assumption that the sample is entirely free from anion ordering, i. e. that $V = 0$. Since one cannot exclude that even for the fastest quenchings some residual anion ordering with a finite, presumably small, value of anion potential $V = V_{\text{res}} > 0$ remains, the above estimate gives an upper limit for t'_b in $(TMTSF)_2ClO_4$.

Choosing this value of t'_b , assuming that $V = 0$ in the quenched samples, and expecting that V increases monotonously with the cooling rate (e. g. in measurements from Refs. [2, 3]), we come to the dashed line on Fig. 3(c) as a fitting curve for $(TMTSF)_2ClO_4$. This enables the estimation of the lower and upper limit for V in the relaxed salt. The latter follow from the width of the region where SDW phases do not exist, $0.1 < V(\text{relaxed } ClO_4)/t_b < 1.6$.

In conclusion, we have shown that the anion ordering in Q1D metals have some nontrivial consequences even in zero magnetic field. Fundamentally new concepts in this context are the need for a matrix SDW susceptibility in solving the interacting problem, and the subsequent introduction of the *effective bare susceptibilities* that diagonalize this matrix. Namely, all previous approaches to the interacting system with anion ordering used inadequately the Stoner criterion with simple SDW bare magnetic susceptibility [8, 10], or, equivalently, assumed that the order parameter is scalar in the bond–antibond space [5, 11]. Here we showed that the non-diagonal kinetic energy in bond–antibond representation is the one that dictates which effective bare susceptibility defines the Stoner criterion (9). The novel proposition of the present work is the existence of the hybride SDW_{\pm} phase at intermediate values of anion potential. Moreover, we have estimated precisely the lower and the upper limit of V for $(TMTSF)_2ClO_4$ salt.

The next important question is how the magnetic field influences the susceptibilities

$\tilde{\chi}_{1,2}$ given by eq. (8). Since the present matrix RPA is valid for finite magnetic fields as well, it remains to take properly into account the qualitatively more complex content of the kinematic part of the Hamiltonian (4,5). We leave this part of work for future, expecting that the basic physics of the SDW phase in high magnetic fields is indeed that of two instabilities, as proposed already by McKernan et al [9]). More specifically, our analysis suggests that two relevant instabilities could be those appearing at wavevectors $2k_F\hat{\mathbf{a}} + \mathbf{q}_+$ and $2k_F\hat{\mathbf{a}} + \mathbf{q}_-$ on Fig. 2.

Acknowledgments: A. B. acknowledges the support of Université Paris VII during his stay at LPTHE. LPTHE is supported by CNRS as Unité Mixte de Recherche, UMR7589.

-
- [1] See for example: P. M. Chaikin, J. Phys. (France), **I6**, 1875 (1996), and references therein.
 - [2] J. S. Qualls *et al.*, Phys. Rev. B **62**, 12680 (2000).
 - [3] N. Matsunaga *et al.*, Phys. Rev. B **62**, 8611 (2000).
 - [4] The real lattice doubling is more complicated as is shown in: D. Le Pévelen, J. Gaultier, Y. Barrans, D. Chasseau, F. Castet and L. Ducasse, Eur. Phys. J. B**19**, 363 (2001).
 - [5] K. Kishigi *et al.*, J. Phys. Soc. Jpn. **66**, 2969 (1997); Y. Hasegawa *et al.*, *ibid.* **67**, 964 (1998);
 - [6] K. Kishigi, J. Phys. Soc. Jpn. **67**, 3825 (1998).
 - [7] K. Yamaji, J. Phys. Soc. Jpn. **53**, 2189 (1984), Y. Hasegawa and H. Fukuyama, J. Phys. Soc. Jpn. **55**, 3978 (1986), G. Montambaux, Phys. Rev. B **38**, 4788 (1988).
 - [8] L. P. Gor'kov and A. G. Lebed, Phys. Rev. B **51**, 3285 (1995).
 - [9] S. K. McKernan *et al.*, Phys. Rev. Lett. **75**, 1630 (1995).
 - [10] Shu-ren Chang and Kazumi Maki, Phys. Rev. B **34**, 147 (1986).
 - [11] M. Miyazaki *et al.*, J. Phys. Soc. Jpn. **68**, 313 (1999).